Innovation in aortoiliac stenting, an in vitro comparison

E. Groot Jebbink*[ac], P.C.J.M. Goverde[d], J.A. van Oostayen[b], M.M.P.J. Reijnen[a], C.H. Slump[c]
Department of [a]Surgery and [b]Radiology, Rijnstate Hospital, Arnhem, The Netherlands
[c]MIRA Institute for Biomedical Technology and Technical Medicine, University of Twente, The Netherlands
[d]Department of Vascular Surgery, Vascular Clinic ZNA, Antwerp, Belgium

ABSTRACT

Aortoiliac occlusive disease (AIOD) may cause disabling claudicatio, due to progression of atherosclerotic plaque. Bypass surgery to treat AIOD has unsurpassed patency results, with 5-year patency rates up to 86%, at the expense of high complication rates (local and systemic morbidity rate of 6% and 16%). Therefore, less invasive, endovascular treatment of AOID with stents in both iliac limbs is the first choice in many cases, however, with limited results (average 5-year patency: 71%, range: 63-82%). Changes in blood flow due to an altered geometry of the bifurcation is likely to be one of the contributing factors. The aim of this study is to compare the geometry and hemodynamics of various aortoiliac stent configurations in vitro.

Transparent vessel phantoms mimicking the anatomy of the aortoiliac bifurcation are used to accommodate stent configurations. Bare Metal Kissing stents (BMK), Kissing Covered (KC) stents and the Covered Endovascular Reconstruction of the Aortic Bifurcation (CERAB) configuration are investigated. The models are placed inside a flow rig capable of simulating physiologic relevant flow in the infrarenal area. Dye injection reveals flow disturbances near the neobifurcation of BMK and KC stents as well. At the radial mismatch areas of the KC stents recirculation zones are observed. With the CERAB configuration no flow reversal or large disturbances are observed. In conclusion, dye injection reveals no significant flow disturbances with the new CERAB configuration as seen with the KC and BMK stents.

Keywords: Endovascular, occlusive disease, aortic bifurcation, stents, kissing stents, CERAB, radial mismatch, hemodynamics

*e.grootjebbink@utwente.nl; phone 0031 534895305; utwente.nl

1. INTRODUCTION

Aortoiliac occlusive disease (AIOD) can lead to incapacitating claudicatio, due to the build-up of atherosclerotic plaque. Bypass surgery to treat (bilateral) AIOD has unsurpassed patency results (5-year patency: 86%), at the expense of high complication rates, local and systemic morbidity rate of 6% and 16% are reported[1]. Therefore, less invasive, endovascular techniques were developed. The technique includes the simultaneous placement of two stents, one placed in each common iliac artery, which meet in the distal aorta (stents 'kiss' in the aorta). This resulted in shorter hospital stay, lower complication rates and shorter recovery time. Therefore endovascular treatment with the deployment of kissing stents is the first choice in many cases. Furthermore secondary open surgery is still an option in case of failure. Currently, several configurations are available to vascular surgeons and interventional radiologists, using balloon expandable (covered or bare metal) stents, or self expandable bare metal stents. The stents can be placed with high or short protrusion into the aorta. The long term patency of kissing stents is limited: 63% after five years. Various aspects of the configuration may affect patency rates of kissing stents, including the positioning of the stents and the discrepancy between the stented lumen and the aortic lumen, the so-called radial mismatch. The latter may cause flow perturbations and thrombus formation that, in turn, may decrease stent patency. Recently the Covered Endovascular Reconstruction of the Aortic bifurcation (CERAB) was introduced, attempting to overcome the disadvantages of kissing stents[2]. With this technique a covered stent is expanded 15-20 mm above the aortic bifurcation and this stent is proximally adapted to the aortic wall with a larger balloon, thereby creating a cone-shaped stent. Then, two iliac covered stents are placed in the distal conic segment and simultaneously inflated, making a tight connection with the aortic stent, as if were they moulded together, thus simulating a new bifurcation. The aortic cuff covers the free floating proximal ends of the iliac

Medical Imaging 2014: Image-Guided Procedures, Robotic Interventions, and Modeling,
edited by Ziv R. Yaniv, David R. Holmes III, Proc. of SPIE Vol. 9036, 90361X

stents that reside in the distal aorta and might thus prevent unwanted flow perturbations around the protruding part of the stents, guiding the flow into the limbs like a funnel. In previous work we have investigated the static geometric differences between the stent configurations and demonstrated that different configurations indeed lead to large differences in mismatch area and volume [3]. With the application of the CERAB technique a large reduction in radial mismatch can be accomplished, if the limbs are placed inside the cuff. In the present study we have assessed the hemodynamic effects of the radial mismatch. Measurements were performed in three different stent configurations using identical, in vitro, rigid phantoms to mimic the vessel anatomy. Results are discussed in view of the current available theoretical and clinical experience on stent patency in the aortoiliac region.

2. METHODS

The silicon models as developed in previous work by Groot Jebbink (2014, in press) are used to investigate the flow conditions. The previous work describes fabrication techniques, dimensions and used stents in detail.

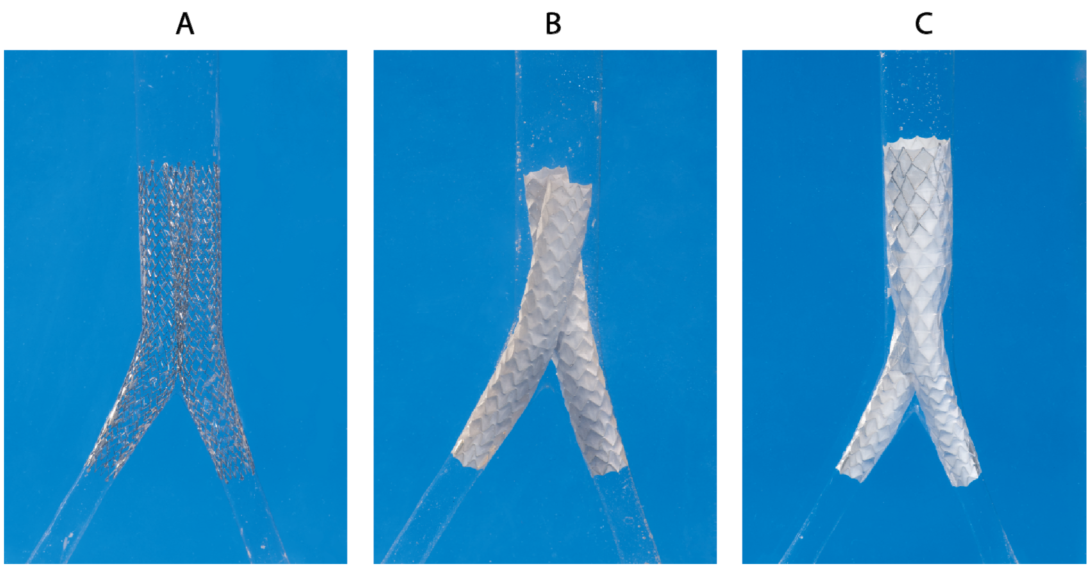

Figure 1. Still colour photographs of the bifurcation model with stents deployed. A: Self expandable nitinol kissing stents. B: Covered balloon expandable kissing stents. C: CERAB configuration.

In order to explore the effects of the stent configurations on blood flow an experimental flow rig was designed to accommodate the flow phantoms. A schematic overview of the flow rig is shown in figure 2; two fully controllable gear pumps are used to generate the flow profile. An inlet section of 1 m (diameter 22 mm) connected to the flow phantom was used to overcome entrance effects caused by the calibre change of the tubing. The renal outflow vessels were connected to the reservoir via a needle valve, to adjust the peripheral resistance. The iliac vessels also incorporate a windkessel to mimic the aortoiliac compliance, again the resistance is controlled using needle valves. The pressure was monitored using a guide wire mounted pressure sensor (PressureWire 5, Radi, Sweden). The flow was monitored with an ultrasonic flow meter (UF8B, Cynergy3). Both the motor control and the sensor readings were managed with Matlab (2012A, The MathWorks Inc., Natick, MA).

Studies were carried out under simulated resting condition at a heart rate of 60 beats/min and a mean suprarenal aortic flow rate of 1.6 l/min with equal outflow of 400 ml/min in each of the renal and iliac arteries. These values are in the physiological range and are comparable to those used in other in vitro studies [4, 5]. The flow profile is based on work from Lee and Chen (2003), they proposed an equation to describe the pulsatile flow pattern recorded in the suprarenal aorta (black line, depicted in figure 4 A). The blood mimicking fluid consisted of a solution of water and glycerol (ratio 44:56 w/w), with a viscosity of 4.5 cP. Besides simulating the viscosity of blood this ratio provides correct matching of the refractive index of the silicone and fluid [6]. This way the dye streams can be imaged accurately. The pressure

aortoiliac waveforms were based on a numeric study performed by Olufsen et al. (2000) and are presented in figure 4 B (black line).
The dye streamlines were recorded at 210 frames per second (A100 camera, Casio). For synchronisation purposes a LED is placed in the field of view, the LED blinks at the start of every cardiac cycle. The LED intensity was tracked and peaks were marked as the start of a new cycle. This aligns the start of a cycle in the video and the start of a new cycle at the control unit. To visualise the flow inside the covered stents, the ePTFE cover was replaced with a transparent cover. The bare metal stents were dipped in a solution of thermoplastic polyurethane (Tecoflex, Thermodics Inc., USA) in dimethylacetamide (8 % w/w), this method was adapted from Chong et al. (2004). Figure 3 A shows the original stent with the PFTE coating, figure 3 B shows the results after applying a transparent coating.

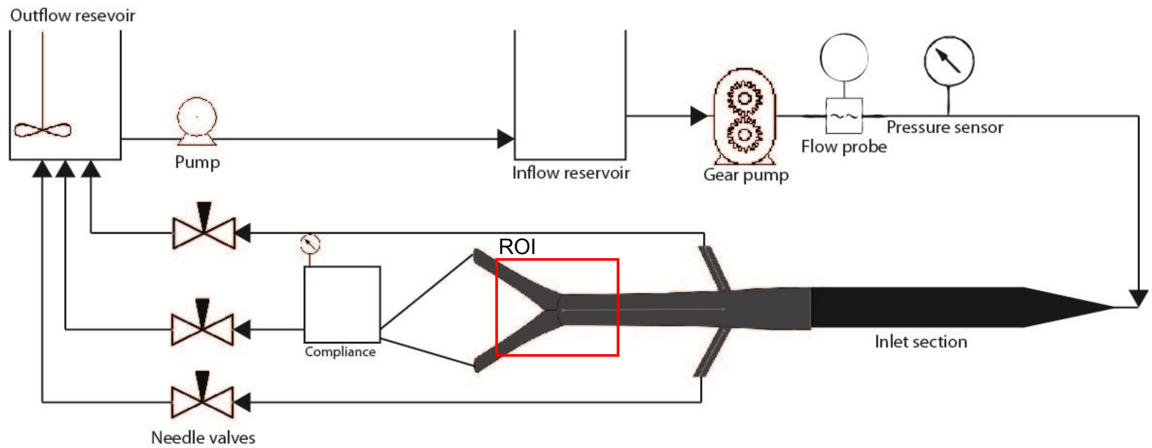

Figure 2. Overview of the flow circuit. Region of interest (ROI) is indicated by the square, recordings of the dye injection (figure 5 and 6) were obtained within this area.

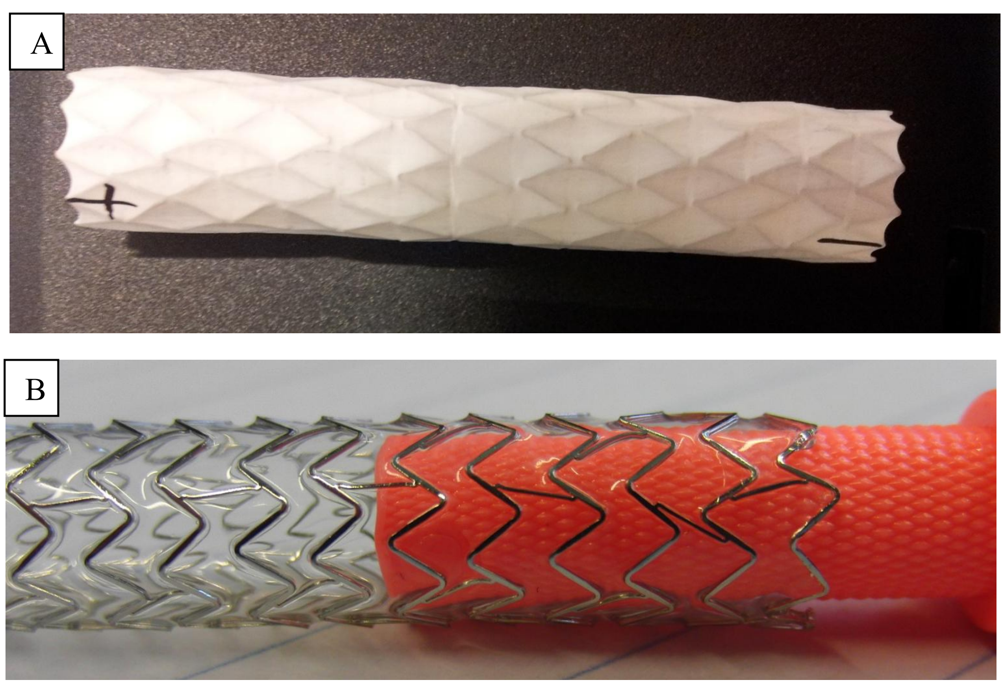

Figure 3. A: stent with original PTFE coating. B: stent after application of a transparent coating.

3. RESULTS

3.1 Influence of the polyurethane cover

To obtain optical access to the flow inside the stented lumen the PTFE cover was replaced with a translucent polyurethane cover. Thereafter the stents were deployed in the vessel phantoms according to protocol by a vascular surgeon (MR). To compare the position and sealing of the polyurethane covered stents and PTFE covered stents a CT scan was obtained from both models, this revealed no differences between both geometries.

3.2 Flow conditions

Figure 4 A compares the flow waveform as sent to the motor (black line) controller and the waveform obtained with the flow sensor (red line). The maximal systolic flow is reached slightly before the intended maximum, the diastolic minimum is not completely met, overall there is good accordance between the two waveforms. Figure 4 B presents the pressure recordings from the model, obtained just above the bifurcation (red line), the black line presents a waveform obtained just above the bifurcation using numerical simulation [7]. The pressure waveforms are in good agreement, only during the diastolic period the plateau phase is not present at 3.8 s. The slope of both the rise and fall in pressure are comparable. The Reynolds number (Re) for continuous flow at the entrance of the model was 385, with a mean flow of 1.6 l/min, vessel diameter 0.022 m, mean flow velocity 0.13 m/s, fluid density 1100 kg/m³ and dynamic viscosity (μ) of 4.5 cP. The Reynolds number at peak pulsatile flow (3.5 l/min) was 868. The Womersley parameter (α) at the inflow section was 13.8.

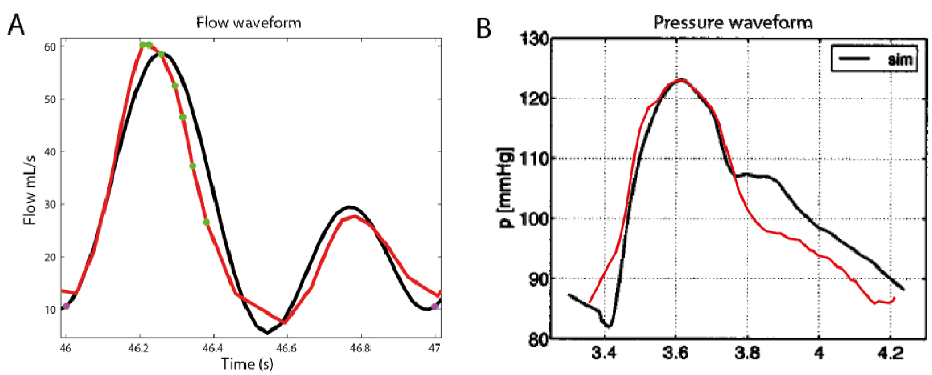

Figure 4. A: Suprarenal flow waveform, the green dots indicate that the feedback loop was active. Purple dots indicate start and end of the cycle. Flow waveform, in red the waveform obtained with the ultrasonic flow sensor. In black the waveform calculated and used to control the pumps. B: Pressure waveform at the bifurcation. In black the waveform obtained from numerical simulations and in red the waveform obtained from the pressure catheter installed just above the bifurcation.

3.3 Local flow perturbations

Under pulsatile flow conditions the maximal systolic flow and minimal systolic flow are visualised using dye injection (figure 5 and 6). The observed dye patterns are enhanced manually offline with the use of white signing. In the upper right corner of each figure the current position in the cardiac cycle is depicted.
The streak lines recorded during maximal systolic flow are depicted in figure 5. For the baseline model laminar flow is recorded during maximal systolic velocity (figure 5 A). This is also holds for the BMK and CERAB configuration. Only for the KC (figure 5 C) stents a recirculation zone is observed at the entrance of the mismatch area. The flow is directed towards the vessel wall and recirculation occurs in both the proximal and distal directions. As the cycle advances the circulation zone displaces more proximally (direction of red arrow, figure 5 C) into the aorta and a large back flow component along the aorta wall is seen (figure 5 C). In the baseline vessel phantom (6 A) a recirculation zone is seen near the vertex of the bifurcation. In the model with BMS stents deployed (6 B) the flow near the kissing part of the stents flows through the stent mesh (from point 1 to 2) and recirculates behind it. In the CERAB configuration (6 D) no deviations from the laminar flow pattern can be discerned using dye injection, no recirculation inside the aortic cuff was observed.

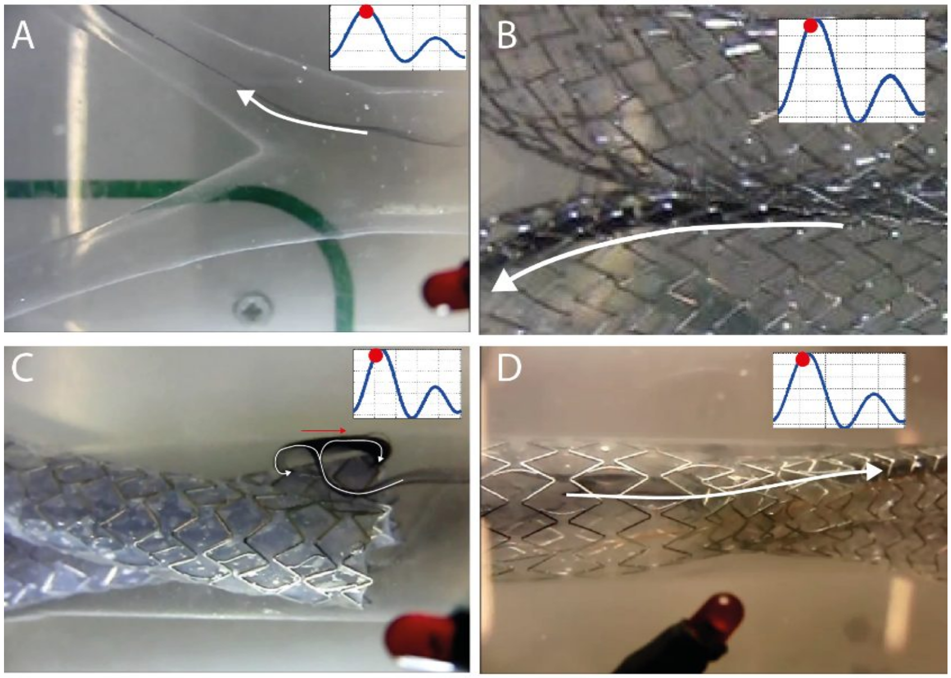

Figure 5. Flow direction is from right to left, dye injection at maximal systolic flow. A: no stents placed, B: bare metal nitinol stents, C: covered bare metal stents, D: CERAB configuration.

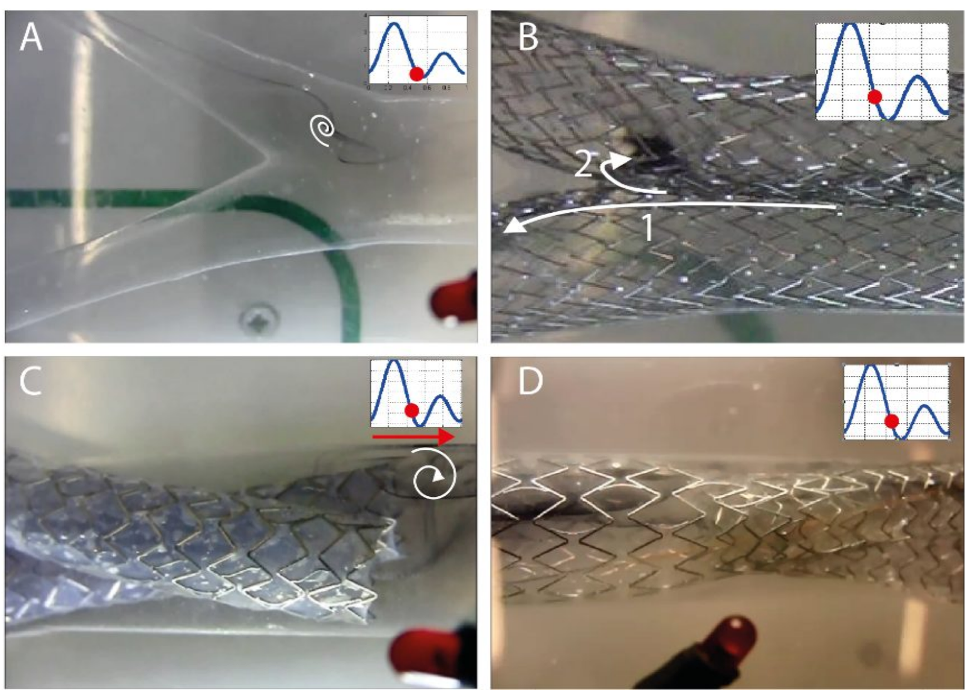

Figure 6. Flow direction is from right to left, dye injection at minimal systolic flow. A: no stents placed. B: bare metal nitinol stents. C: covered bare metal stents. D: CERAB configuration.

4. DISCUSSION

The baseline results (no stents) of the current study are in accordance with results obtained in earlier studies, in particular the undisturbed flow at maximal systolic flow and the recirculation zone observed at the vertex during the diastolic phase (maximal deceleration) [8, 9]. The accordance of reverse flow is also in accordance with reported in vitro and in vivo results [10]. Furthermore, results of our current study indicate that stents placed at the aortoiliac bifurcation in a kissing configuration can perturb the blood flow locally. In particular the mismatch zones created when kissing covered stents protrude into the aorta cause recirculation at the proximal in flow of the stents. The BMK stents cause recirculation near the apex of the bifurcation. Previous studies point at the benefit of using covered stents instead of bare metal stents, because stent induced alterations in shear stress cannot trigger ingrowth of hyperplastic tissue [11]. However, the application of the PTFE cover may cause more extensive flow perturbations near the inflow because a stagnant blood column can form in the mismatch area. The resulting recirculation along the aortic wall may influence local wall shear stress levels. Especially lowering of the shear stress can cause reactions and thickening of the wall shear stress, resulting in edge stenosis and stent failure. Hughes et al (2006) concluded that the use of bare metal nitinol stents may be preferred above bare metal balloon-expandable stents, because of the reduction in mismatch area. Our previous study also supports these results [3]. To our knowledge no clinical data is available comparing balloon-expandable stents with self-expandable nitinol stents. Combining both features, reduction in mismatch area and application of a cover, as is done in the CERAB configuration might yield better patency results. Concerning the mismatch results, using dye injection no flow perturbations could be observed at the changeover between the aortic cuff and the iliac limbs of the CERAB configuration. This study mainly focusses on influences of radial mismatch on flow, several studies consider this an important factor influencing stent patency [12-14]. However, there is still room for further research to proof this undisputable.

The vascular models used in this experiment could also influence the obtained results, because they are rigid in contrast to the elastic behavior of arteries in vivo. Moore et al (1992) already showed that the resulting flow profile and sites of recirculation are not strongly affected when comparing rigid and compliant models. Though it can influence the absolute wall shear stress. Furthermore the elasticity of the vessel wall has deteriorated significantly in patients with heavily calcified lesions, this is also the patient category suitable for kissing stent placement. This reduces the need for a very elastic model.

The current in vitro setup is based on a two element lumped parameter model (compliance and resistance). An admitted limitation to the model is the absence of a correct relation between the pressure and flow waveforms, the modulation and phase at higher frequencies do not resemble physiologic data [15]. Implementing a three element lumped parameter model would increase this correlation considerably. This also limits the usability of obtained pressure readings when applying a certain flow waveform. Currently simulations are performed under resting conditions, however, it is known that distribution of blood between de renal vessels and the iliac vessels changes when exercising. This might also influence the observed results. The flow visualization technique, dye injection, only reveals one streamline or a whole group of streamlines at a time. The application of techniques that reveal more temporal and spatial information, for instance PIV techniques with laser or ultrasound could result in a better understanding of the local flow phenomena. Furthermore this would enable the quantification of wall shear stress in the area of flow disturbances.

5. CONCLUSION

As shown before, different stent configurations have different geometrical effects. The current flow study, using dye injection, indicates that these geometries have different effects on the local flow patterns. The mismatch area that is present between de vessel wall and stent wall of de KC stents causes recirculation zones at the proximal inflow area. This could potentially limit the patency of the stent configuration. With the CERAB configuration such recirculations could be observed, indicating that the aortic cuff effectively seals the mismatch area.

[1] K. W. Chiu, R. S. Davies, P. G. Nightingale *et al.*, "Review of direct anatomical open surgical management of atherosclerotic aorto-iliac occlusive disease," Eur J Vasc Endovasc Surg, 39(4), 460-71 (2010).

[2] P. Goverde, F. Grimme, P. Verbruggen *et al.*, "Covered endovascular reconstruction of aortic bifurcation (CERAB) technique: a new approach in treating extensive aortoiliac occlusive disease," The Journal of cardiovascular surgery, 54(3), 383-387 (2013).

[3] E. Groot Jebbink, F. A. B. Grimme, P. C. J. M. Goverde *et al.*, "Geometrical consequences of kissing stents and the Covered Endovascular Reconstruction of the Aortic Bifurcation configuration in an in vitro model for endovascular reconstruction of aortic bifurcation," Journal of Vascular Surgery, (2014, in press).

[4] J. E. Moore, Jr., D. N. Ku, C. K. Zarins *et al.*, "Pulsatile flow visualization in the abdominal aorta under differing physiologic conditions: implications for increased susceptibility to atherosclerosis," J Biomech Eng, 114(3), 391-7 (1992).

[5] C. K. Chong, T. V. How, and P. L. Harris, "Flow visualization in a model of a bifurcated stent-graft," J Endovasc Ther, 12(4), 435-45 (2005).

[6] M. Y. Yousif, D. W. Holdsworth, and T. L. Poepping, "Deriving a blood-mimicking fluid for particle image velocimetry in Sylgard-184 vascular models," Conf Proc IEEE Eng Med Biol Soc, 2009, 1412-5 (2009).

[7] M. S. Olufsen, C. S. Peskin, W. Y. Kim *et al.*, "Numerical simulation and experimental validation of blood flow in arteries with structured-tree outflow conditions," Ann Biomed Eng, 28(11), 1281-99 (2000).

[8] S. Fabregues, K. Baijens, R. Rieu *et al.*, "Hemodynamics of endovascular prostheses," Journal of Biomechanics, 31(1), 45-54 (1998).

[9] E. M. Pedersen, H. W. Sung, A. C. Burlson *et al.*, "Two-dimensional velocity measurements in a pulsatile flow model of the normal abdominal aorta simulating different hemodynamic conditions," Journal of Biomechanics, 26(10), 1237-47 (1993).

[10] R. Holenstein, and D. N. Ku, "Reverse flow in the major infrarenal vessels--a capacitive phenomenon," Biorheology, 25(6), 835-42 (1988).

[11] S. S. Sabri, A. Choudhri, G. Orgera *et al.*, "Outcomes of Covered Kissing Stent Placement Compared with Bare Metal Stent Placement in the Treatment of Atherosclerotic Occlusive Disease at the Aortic Bifurcation," Journal of Vascular and Interventional Radiology, 21(7), 995-1003 (2010).

[12] M. B. Saker, W. F. Oppat, S. A. Kent *et al.*, "Early failure of aortoiliac kissing stents: histopathologic correlation," J Vasc Interv Radiol, 11(3), 333-6 (2000).

[13] A. Greiner, H. Muhlthaler, B. Neuhauser *et al.*, "Does stent overlap influence the patency rate of aortoiliac kissing stents?," J Endovasc Ther, 12(6), 696-703 (2005).

[14] M. J. Sharafuddin, J. J. Hoballah, T. F. Kresowik *et al.*, "Long-Term Outcome following Stent Reconstruction of the Aortic Bifurcation and the Role of Geometric Determinants," Annals of Vascular Surgery, 22(3), 346-357 (2008).

[15] N. Westerhof, J. W. Lankhaar, and B. E. Westerhof, "The arterial Windkessel," Medical & Biological Engineering & Computing, 47(2), 131-141 (2009).